Li et al. EURASIP Journal on Wireless Communications and Networking (2016) 2016:161
DOI 10.1186/s13638-016-0648-7

EURASIP Journal on Wireless Communications and Networking

RESEARCH Open Access

High-efficiency and low-consumption underwater sonar transmitter with improved triple-pulse HP-PWM signal model based on class D amplifier

Yanchao Li, Fajie Duan*, Jiajia Jiang and Xianquan Wang

Abstract

An improved triple-pulse high-power pulse-width modulation (HP-PWM) signal model is proposed to enhance the performance of current underwater sonar transmitter. The presented model is based on reducing the third and fifth harmonic energy of the HP-PWM signal. The achievement of low-power consumption has been implemented using class D amplifier and high-quality factor (High-Q) underwater acoustic transducer (UAT). High efficiency is demonstrated by simulations (reducing 41 % of the third and fifth harmonic energy). Feasibility of the presented model under different conditions has been proved by experiments.

Keywords: Audio frequency power amplifiers, Pulse-width modulation, Continuous wave, Class D amplifier

1 Introduction

Forward-looking sonar system is a common underwater communication technology of wireless sensor network [1–3]. Reducing power consumption in audio frequency power amplifiers (AFPAs) [4] of forward-looking sonar system [5] remains a great challenge. Some solutions are proposed to solve this problem, such as GaN-based gate driver circuit and power conditioning circuit [6]. These solutions need extra hardware design based on pulse-width modulation (PWM) [7] to improve the efficiency of AFPA. Therefore, the design of the PWM signal model appears to be another important branch of many investigations [8].

For forward-looking sonar system, underwater sonar transmitter is an acoustic beam generator, and its performance directly determines the detection range and measuring accuracy of sonar equipment. The transmitter includes signal generator, power amplifier circuit, and acoustic transducer. Among them, the power amplifier circuit needs the maximum power consumption. However, recent system cannot achieve both high performance and low power consumption at the same time. Thus, the combination of PWM signal and underwater sonar transmitter remains to be an investigation to solve this above problem.

One key process encountered in the design of the PWM signal model concerns the selection of pulse driving form. In general, there are two forms for PWM signal: one is continuous wave (CW) pulse signal with fixed frequency and amplitude and the other is a linear frequency modulation (LFM) pulse signal whose frequency is time varying. In comparison of the above two forms, the CW pulse signal is more practical than LFM. Besides, due to the fast response and high efficiency of class D amplifier [9–14], CW pulse signal can be driven with high precision in power amplifier system. Consequently, the PWM signal model remains to be designed for low power consumption and high efficiency.

In this paper, an improved triple-pulse HP-PWM signal model based on class D amplifier is presented for AFPA of underwater sonar transmitter. This letter highlights our recent work on this topic and focuses on the enhancement of power consumption efficiency.

* Correspondence: fjduan@tju.edu.cn
State Key Lab of Precision Measuring Technology and Instruments, Tianjin University, Tianjin 300072, China

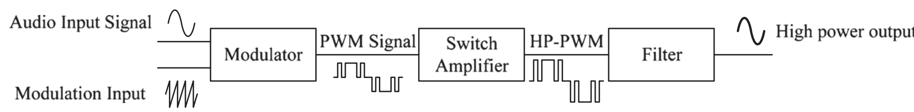

Fig. 1 Structure of class D amplifier

2 Background of class D amplifier used in underwater sonar transmitter

As is shown in Fig. 1, class D amplifier is basically composed of three parts. The first part is a modulator consisted of comparator and triangular wave generator. In the positive input of comparator, audio input signal with a certain DC bias is required to be placed there, and a high frequency triangle wave, whose frequency is typically ten times more than the audio input signal, is connected to the negative input. The output of comparator is the desired PWM signal.

The second part is a switch amplifier, which is a large current switch controlled by PWM signal. It transforms the PWM signal into HP-PWM signal.

The last part is to recover the sound signal from the HP-PWM signal. A low-pass or band-pass filter is applied to achieve this function. The cut-off frequency is set near frequency of amplified audio signal. Then, the higher harmonics are eliminated and fundamental frequency of audio signal is reserved.

In this paper, the HP-PWM signal drives an underwater acoustic transducer (UAT) with a fixed operation frequency and High-Q (as shown in Fig. 2). To achieve the ultrasonic frequency, modulation frequency of HP-PWM signal should reach at least ten times to avoid large total harmonic distortion (THD). And it is important to select an appropriate HP-PWM signal model which can reduce the modulation frequency and suppress the high harmonic component simultaneously.

3 Single-pulse model of HP-PWM signal

The simplest HP-PWM modulation is using a single-pulse model in half a cycle as shown in Fig. 3.

As $f(x)$ is an even function, the sine coefficient is zero after Fourier expansion. Cosine coefficient a_n is the amplitude of the nth harmonic as follows:

$$a_n = \frac{1}{\pi}\int_{-\pi}^{\pi} f(x)\cdot cos(nx)dx = \frac{4}{n\pi}sin(n\theta) \quad (1)$$

where θ is the half pulse width and n is the odd harmonic order.

According to the definition of energy, the total energy E in a period of the proposed HP-PWM pulse is 4θ, and the harmonic energy E_n can be expressed as

$$E_n = \int_{-\pi}^{\pi}(a_n cosx)^2 dx \quad (2)$$

Substituting a_n into the Formula (2), E_n converts to

$$E_n = \left[\frac{4}{n\pi}sin(n\theta)\right]^2\cdot\pi \quad (3)$$

To weaken the energy of high harmonic components, ratio η_n of the harmonic energy E_n to the total energy E should be as small as possible. η_n can be expressed as

$$\eta_n = \frac{E_n}{E} = \frac{\left[\frac{4}{n\pi}sin(n\theta)\right]^2\cdot\pi}{4\theta} = \frac{4sin^2(n\theta)}{n^2\pi\theta} \quad (4)$$

when the half width of the pulse is lower than 0.4 rad, the fundamental harmonic energy is less than 50 % of the total energy.

4 Improved triple-pulse model of HP-PWM signal

In order to solve the defects of the third and fifth harmonic energy in the single-pulse model, a triple-pulse model is proposed by adding two narrow pulses with a symmetrical relative to the original signal-pulse model, which is shown in Fig. 4.

The broad half pulse width Δ_1, narrow half pulse width Δ_2, and their spacing α are in accordance with the following relations:

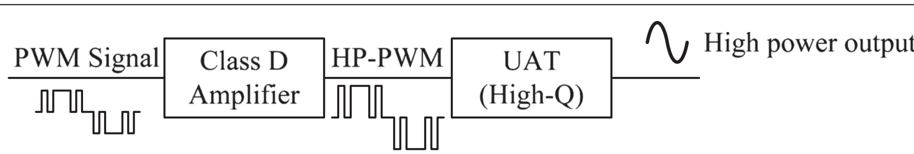

Fig. 2 Structure of underwater sonar transmitter

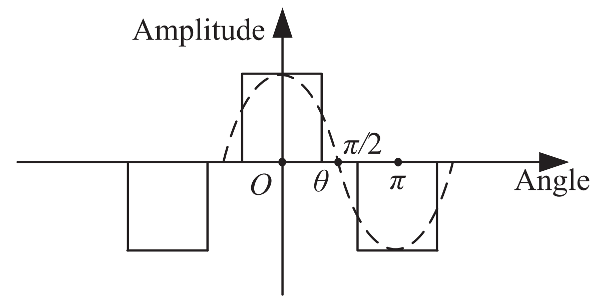

Fig. 3 Single-pulse model of HP-PWM signal

$$\frac{\Delta_1}{\Delta_2} = \frac{1}{cos\alpha} \tag{5}$$

As the signal is still an even function, the cosine coefficient after Fourier expansion is as follows:

$$a_n = \frac{4}{n\pi}[sin(n\Delta_1) + 2cos(n\alpha)sin(n\Delta_2)] \tag{6}$$

Harmonic energy E_n is

$$E_n = \frac{16}{n^2\pi}[sin(n\Delta_1) + 2cos(n\alpha)sin(n\Delta_2)]^2 \tag{7}$$

and the total energy E is $4\Delta_1 + 8\Delta_2$. Ratio η_n of E_n to E is

$$\eta_n = \frac{E_n}{E} = \frac{\frac{4}{n^2\pi}[sin(n\Delta_1) + 2cos(n\alpha)sin(n\Delta_2)]^2}{\Delta_1 + 2\Delta_2} \tag{8}$$

Substituting Formula (7) into Formula (8), η_n can be exchanged by

$$\eta_n = \frac{4[sin(n\Delta_1) + 2cos(n\alpha)sin(n\Delta_1 cos\alpha)]^2}{n^2\pi\Delta_1(1 + 2cos\alpha)} \tag{9}$$

5 Simulations

The purpose of simulations is to verify the feasibility of the proposed model. Firstly, for the single-pulse model of the HP-PWM signal, ratios of fundamental wave to total energy and the sum of the third and fifth harmonics to the total energy are compared to illustrate the infeasibility of this model.

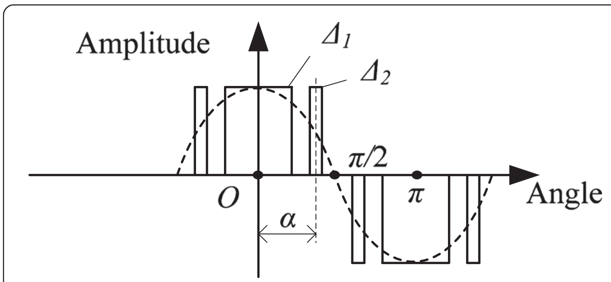

Fig. 4 Improved triple-pulse model of HP-PWM signal

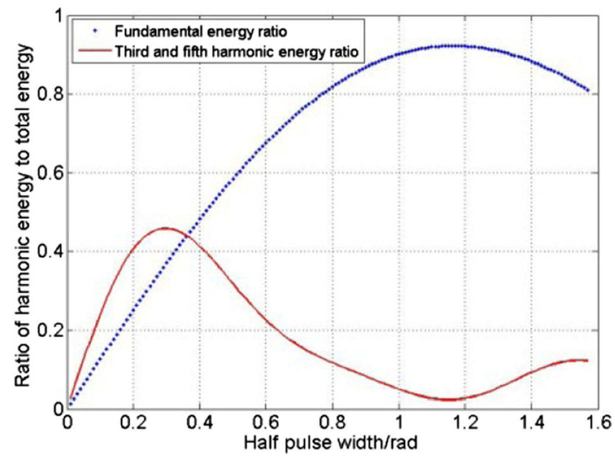

Fig. 5 Efficiency under different conditions for single-pulse model of HP-PWM signal

Figure 5 shows the results of simulation in the form of the single-pulse model. The fundamental energy varied greatly with the change of pulse width. If θ is less than 0.4 rad, the fundamental energy is less than 50 % of the total energy. The sum of the third and fifth harmonics is available only if θ is between 0.8 and 1.4 rad. When θ is less than 0.6 rad, the efficiency of the third and fifth harmonic energy can reach 45 %, and the final high power output will be affected seriously by the third and fifth harmonic energy.

Secondly, for improved triple-pulse model of the HP-PWM signal, the simulations are illustrated in Fig. 6. The results show that the ratio of fundamental energy to total energy has a wide feasible region under the condition that Δ_1 is greater than 0.2 rad, which is much better compared with the results of single-pulse model. The ratio of the third and fifth harmonic energy to total energy has small proportion under the condition of $\alpha \in [0.6, 1]$ and $\Delta_1 \in [0, 0.6]$, as well as $\alpha \in [1.2, 1.57]$ and $\Delta_1 \in [0.7, 1.57]$. When α is 0.79 rad, it reaches 4 %, which is 41 % lower than the single-pulse model. The result of Fig. 7 shows that there are two extreme points, which are $[\alpha, \Delta_1] = [0.79, 0.1]$ and $[1.41, 0.91]$. It is obvious that the extreme point $[\alpha, \Delta_1] = [0.79, 0.1]$ is the optimal solution for low power consumption system by the proposed triple-pulse model.

6 Experiments

To verify the validity of the proposed model, a test platform was constructed as shown in Fig. 8. The test

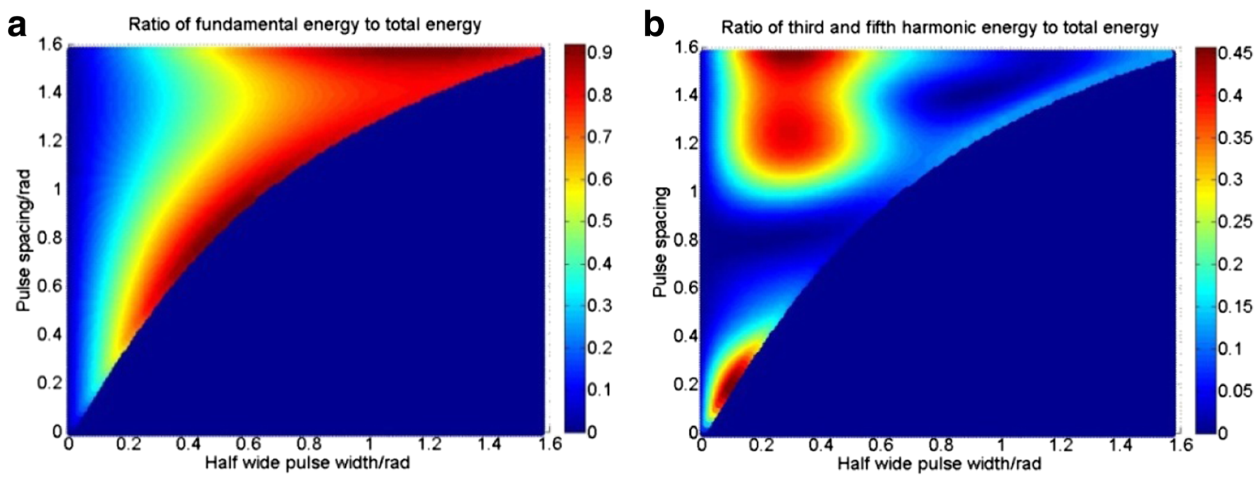

Fig. 6 Efficiency under different power consumptions for improved triple-pulse model of HP-PWM signal. **a** Ratio of fundamental wave to total energy. **b** The sum of the third and fifth harmonics to total energy

platform consisted of a HP-PWM signal generation system, two underwater acoustic transducers, and a large water tank. The HP-PWM signal generation system included field programmable gate array (FPGA) and improved class D amplifier. Through the program module designed in the FPGA, the designed PWM signal with high precision was generated as signal input of class D amplifier *HV7350* produced by Microchip Technology Incorporated. The frequency and peek-to-peek value of the required HW-PWM signal were 200 KHz and 120 V. The center frequency of the underwater acoustic transducer is also 200 KHz, and the quality factor is 5.0. The parameters of the proposed triple-pulse model are set as the values of simulations, where $\alpha = 0.79$ and $\Delta_1 = 0.1$. Finally, the HW-PWM signal is illustrated in Fig. 9.

Then, the distance between transmitting and receiving transducers was 40 cm, and as the underwater speed of sound is about 1500 m/s, the signal transmission time from transmitter to receiver was about 280 μs. The broad half pulse width Δ_1 was set five values from 0.06 to 0.14 and the spacing α were set from 0.75 to 0.83. The amplitudes of the receiving signal on the underwater acoustic transducer are shown in Table 1.

Through the results of Table 1, it is obvious that the proposed triple-pulse model of HP-PWM signal

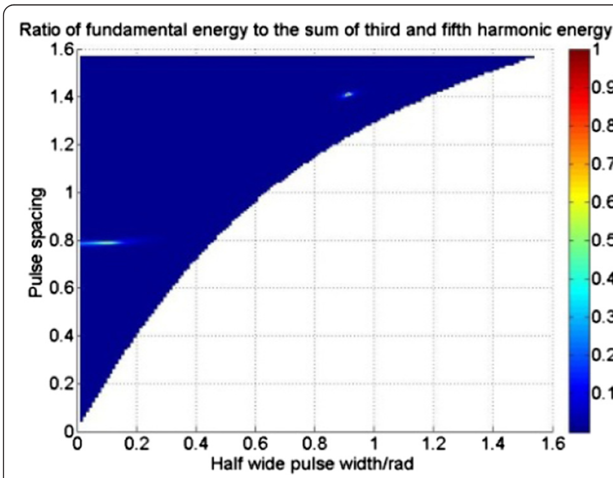

Fig. 7 Ratio of fundamental wave to the sum of the third and fifth harmonics one

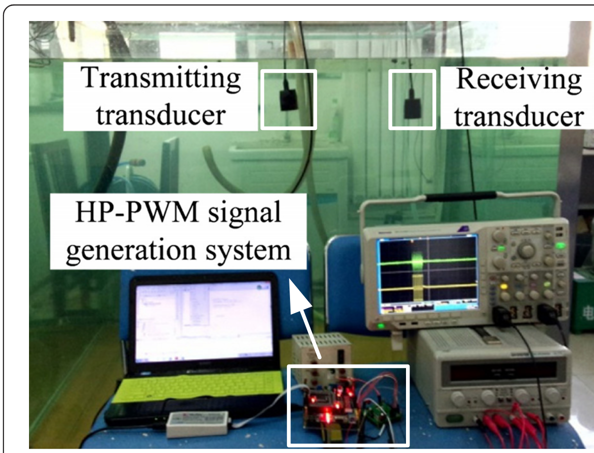

Fig. 8 Structure of test platform

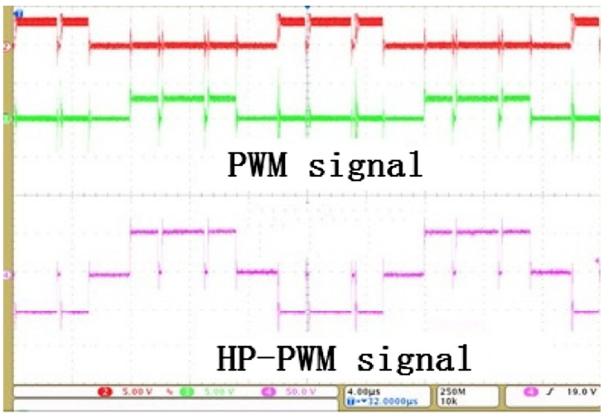

Fig. 9 Waveforms of PWM and HW-PWM signals

can basically achieve the performance of theoretical analysis. When α is 0.79 rad, the amplitudes of the receiving signal can reach the maximum value. Then, the output power can be easily controlled by adjusting Δ_1. It indicates that the proposed model can improve the efficiency and performance of underwater sonar transmitter under the condition of low power consumption.

7 Conclusions

This paper has proposed an improved triple-pulse model of HP-PWM signal to enhance the efficiency of power amplifier circuit in sonar transmitter system under the condition of low power consumption, which reduces 41 % of the third and fifth harmonic energy. The strategies are based on improving the driving model of power amplifier circuit and combining the features of underwater acoustic transducer to achieve a sonar transmitter system with high efficiency and low power consumption. Confirmatory simulations and experimental results are provided to highlight the feasibility of proposed model.

Table 1 Amplitudes of receiving signal under different conditions

Broad half-pulse width/rad	0.06	0.08	0.10	0.12	0.14
Amplitude of the receiving signal ($\alpha = 0.75$)/mv	67.5	126.9	203.3	282.6	403.6
Amplitude of the receiving signal ($\alpha = 0.77$)/mv	72.5	137.2	212.5	300.3	408.6
Amplitude of the receiving signal ($\alpha = 0.79$)/mv	78.5	142.5	213.8	315.3	425.9
Amplitude of the receiving signal ($\alpha = 0.81$)/mv	66.7	122.8	194.3	275.1	386.0
Amplitude of the receiving signal ($\alpha = 0.83$)/mv	63.8	117.8	186.5	257.8	370.7

Competing interests
The authors declare that they have no competing interests.

Acknowledgements
This work was supported by the Marine Economic Innovation and Development Project of China under Grant No.CXSF2014-2, the National Natural Science Foundation of China under Grant No.51275349, the China New Century Excellent Talents under Grant NECT, the China Tianjin Science and Technology to support key projects under Grant No.11ZCKFGX03600, and the China Tianjin Science and Technology Sea Project under Grant No.KX2010-0006. The authors declare that they have no competing interests.

Received: 29 March 2016 Accepted: 23 May 2016
Published online: 07 July 2016

References
1. Q Liang, Radar sensor wireless channel modeling in foliage environment: UWB versus narrowband. IEEE Sensors J. **11**(6), 1448–1457 (2011)
2. H Shu, Q Liang, J Gao, Wireless sensor network lifetime analysis using interval type-2 fuzzy logic systems. IEEE Trans. Fuzzy Syst. **16**(2), 416–427 (2008)
3. Q Liang, Q Ren, Energy and mobility aware geographical multipath routing for wireless sensor networks. IEEE Communications Society **3**,1867–1871(2005)
4. M Kiwanuka, Variations on the complementary folded cascade transimpedance stage in discrete audio frequency power amplifiers. Electronics World **119**(1931),26–37(2013)
5. S Haniotis, P Cervenka, C Negreira et al., Seafloor segmentation using angular backscatter responses obtained at sea with a forward-looking sonar system. Appl. Acoust. **89**,306–319(2015)
6. A Delias, A Martin, P Bouysse et al., Low consumption and high frequency GaN-based gate driver circuit with integrated PWM. Electron. Lett. **51**(18),1415–1416(2015)
7. VME Antunes, VF Pires, JFA Silva, Narrow pulse elimination PWM for multilevel digital audio power amplifiers using two cascaded H-bridges as a nine-level converter. IEEE Transactions on Power Electronics **22**(2),425–434(2007)
8. AC Floros, JN Mourjopoulos, Analytic derivation of audio PWM signals and spectra. J. Audio Eng. Soc. **46**(7–8),621–633(1998)
9. F Chierchie, EE Paolini, L Stefanazzi et al., Simple real-time digital PWM implementation for class-D amplifiers with distortion-free baseband. IEEE Trans. Ind. Electron. **61**(10),5472–5479(2014)
10. J Lu, H Song, R Gharpurey, A CMOS class-D line driver employing a phase-locked loop based PWM generator. IEEE J. Solid State Circuits **49**(3),729–739(2014)
11. CK Lam, MT Tan, SM Cox et al., Class-D amplifier power stage with PWM feedback loop. IEEE Transactions on Power Electronics **28**(8),3870–3881(2013)
12. SM Cox, CK Lam, MT Tan, A second-order PWM-in/PWM-out class-D audio amplifier. IMA J. Appl. Math. **78**(2),159–180(2013)
13. CW Lin, BS Hsieh, Dynamic power efficiency improvement for PWM class-D amplifier. IEICE Electronics Express **10**(6),1-6(2013)
14. T Ge, JS Chang, Modeling and technique to improve PSRR and PS-IMD in analog PWM class-D amplifiers. IEEE Transactions on Circuits and Systems II-Express Briefs **55**(6),512–516(2008)